Proc. Indian Acad. Sci. (Engg. Sci.) Vol. 4, Pt. 1, April 1981, pp. 75–85. © Printed in India.

Gigawatt power electron beam generator

K K JAIN and P I JOHN
Physical Research Laboratory, Ahmedabad 380 009

MS received 12 August 1980; revised 24 January 1981

Abstract. In this paper, the design and constructional details of a short-pulse electron beam generator are presented highlighting some of the novel features of its operation. The diagnostic results of the electron beam, both in the diode and in the drift region, are described. A 60-ns duration 200 keV, 30 kA electron beam has been obtained.

Keywords. Relativistic electron beam; pulse power techniques; plasma heating.

1. Introduction

There has been a rapid development since the early 1960s of new pulsed high-power sources. In 1962, J C Martin initiated the development of high-pulsed power systems at the Atomic Weapon Research Establishment in England. He successfully combined the existing Marx generator technology with transmission line techniques to produce sub-microsecond duration high-power pulses. Since then the technology of pulse power generators has advanced to the level where it is now possible to produce terrawatt power electron beams for times of the order of a few tens of nanoseconds. In addition to the developments in high-power pulse technology, there have been in the past several years intensive efforts to exploit the unique attributes of the intense relativistic electron beam, which have been used for microwave generation (Nation 1970), laser pumping (Bagratashoili *et al* 1973), collective ion acceleration (Grabill & Uglum 1970), x-ray production and generation of shock waves in targets (Oswald *et al* 1966).

The high power and high currents carried by these beams are of special interest in the heating (Sandel 1973) and confinement of plasmas. The E-beam heated linear solenoid is a recent example. Laminar beams (beam propagating along the magnetic field) have shown nonclassical energy deposition in plasma. Recent theoretical studies (Chu & Rostoker 1974; Molvig & Rostoker 1977) have shown that if the beam is rotated such that a substantial component of the beam energy is in the rotational component, fast magnetic perturbations can be induced in the plasmas, whereby cross field plasma currents can be driven which can heat the ion component more efficiently than laminar beams. The present device has been constructed to investigate the intense electron beam-plasma interaction in the rotational mode.

Section 2 of this paper contains an overall description and design features of the various components of the generator. Section 3 summarises the diagnostic results of the short-pulse beam produced with the device.

2. Overall description of the device

The electron beam generator consists of (i) a primary energy storage subsystem (ii) a pulse-forming line (iii) a high voltage holding switch (iv) a field emission diode and the drift region. The block diagram of the electron beam generator is shown in figure 1, illustrating the principal components of the generator.

The primary storage element is a twenty-stage one-magavolt Marx generator. It is capable of storing 5 kilojoules of energy in its twenty capacitors each of 0·2 μF capacitance. The stored energy in the Marx is transferred to a second energy storage module, a 4·8 ohm co-axial water dielectric pulse-forming line. The water line gets charged to its peak voltage by the Marx generator in about 600 ns. At this stage, the output switch which is a series combination of a pressurised gas switch and a water switch breaks down. Thus the stored energy in the water line is transferred to a vacuum field emission diode where the beam is generated. By using graphite as the cathode and brass grid as the anode, a 30 kA diode current is obtained when 200 kV is applied between them. The functional diagram of the beam generator is shown in figure 2. The details of the major constituents of the beam generator are described below.

2.1 *Marx generator*

Amongst the many techniques for producing high voltage pulses, the Marx generator is the best known because of its high power output (Fitch 1971; Prestwich 1971). The Marx principle is the transient series connection of a number of electrostatic energy storage modules. The capacitors are charged in parallel *via* the charging

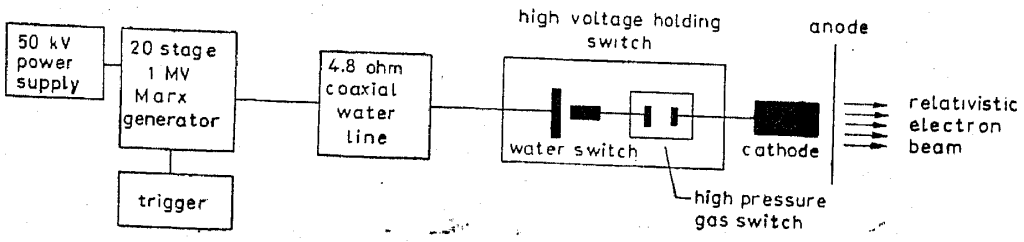

Figure 1. Block diagram of the relativistic electron beam generator

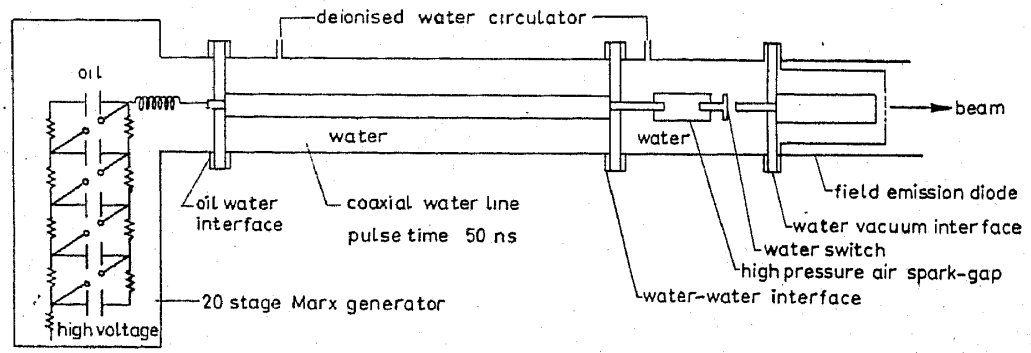

Figure 2. Functional diagram of the relativistic electron beam generator

resistance in the high voltage leg of the circuit while the other side is connected to the ground *via* the ground leg resistor chain. The Marx generator is erected by triggering a series of air spark gaps. When this happens, the low impedance spark gaps effectively connect the capacitors in series. Except for their contribution to voltage grading, the charging and ground leg resistance play virtually no part in the pulse mode. The net voltage achieved with the Marx circuit is simply the charging voltage per stage times the number of stages.

The working of the Marx can be better understood from the schematic of the Marx generator circuit shown in figure 3. The condenser C's connected in parallel are charged to d.c. charging voltage V_0 through resistances Rc's. When they are charged, the first air spark gap G_1 of the circuit is triggered by an external source. This raises the point A to the potential $2V_0$. Then the firing of gap G_2 requires an over voltage across it. The present Marx generator takes advantage of geometrical arrangement for the switching of gap G_2 and the subsequent gaps. In our case, the capacitor C's are arranged as two stacks in zig-zag fashion. So the effective distance between alternate capacitors is less than that between adjacent capacitors. Hence the coupling capacitance C_c between alternate capacitors is now always greater than that between adjacent capacitors. Also in this configuration, because of the small distances between alternate capacitors, their large surface area, and the use of oil as a dielectric between them, the coupling capacitor is larger than the gap-to-ground capacitance C_g (Nation 1979). So when point A is clamped to 2 V_0, the potential at point B is raised to

$$2\,V_o \frac{C_g}{C_0 + C_g}.$$

Therefore the voltage across gap G_2

$$V_{BA} = 2V_0 - 2V_0 \frac{C_g}{C_c + C_g},$$

$$= 2V_0 \frac{C_c}{C_c + C_g};$$

if $C_c \gg C_g$, then

$$V_{BA} = 2V_0.$$

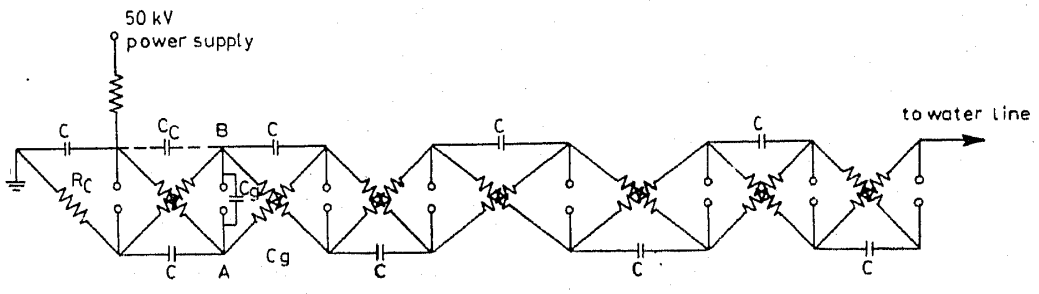

Figure 3. Capacitively coupled $n = 2$ Marx generator circuit.

Hence we can operate the Marx at about 50% of the self-breakdown voltage of the spark gaps.

The assembly of capacitors, air spark gap chamber and charging resistors is immersed in transformer oil in a tank of dimensions approximately $180 \times 75 \times 60$ cm^3. The twenty 0·2 μF 50 kV capacitors are mounted on a cloth fibre structure. Two columns of copper sulphate solution with a 40 kilo ohm resistance each are used as charging resistances. The advantage of using copper sulphate solution as the charging resistance is that it can withstand megavolt stresses and can be made in any convenient shape.

The Marx generator is erected by means of twenty spark gap switches operating in high pressure air, housed inside a common pressure-sealed 1·5 m long chamber. Each spark gap in this chamber is made of brass electrodes of diameter 20 mm while the elctrode gap is 8 mm. The reason for keeping the gap smaller than the diameter is to have a uniform electric field between them as this helps in reliable switching. The spark gaps are housed in a single chamber to provde an efficient optical coupling between various spark gaps. When the first spark gap is triggered, the resulting ultraviolet radiation photoionizes the gas in the gap region of successive gaps and this is sufficient to cause complete triggering of all the gaps. By adjusting the pressure inside the housing chamber, the charging voltage for each capacitor could be adjusted between 15 and 50 kV. These spark gaps are connected to condensers and charging resistor columns. A corona ring is connected at the output end of the Marx where the pulsed high voltage appears. This is shaped in such a way that large electrical stress in any preferential direction is avoided.

The prime requirement of a Marx generator is reliability and very low jitter during erection time, which depends upon the triggering method. Generally, in all the Marx generators (from those producing a few kV to those producing a few MV), the erection of the Marx is achieved by a few trigger spark gaps *i.e.* trigratrons, which requires additional high voltage generators for operation.

To avoid some of these problems, we have tried a trigger generator in the form of a sliding spark source. The spark source consists of two electrodes fixed on the plane of a nylon cylinder, with their tips just projecting on the surface of nylon as shown in figure 4. This trigger source is mounted about 5 cm away from the first air spark gap inside the spark gap chamber and is electrically isolated from the Marx. When a 6 kV

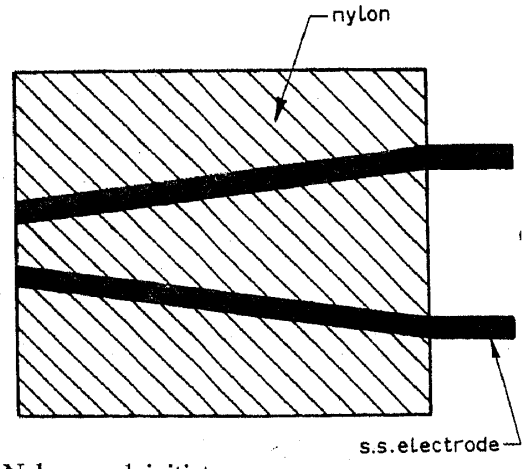

Figure 4. Nylon spark initiator.

voltage is applied between the electrodes, a surface discharge on nylon is developed which emits ultraviolet (UV) radiation. This radiation helps in switching the main spark gaps. The Marx is erected normally at a voltage which is 60–70 % of the value at which the spark gaps fire without the triggering pulse. An unwanted prefire has never been experienced so far.

The capacitors in the Marx generator are charged by a variable 0–50 kV high voltage power supply whose input voltage is varied linearly using a variable auto-transformer coupled to a low rev/min reversible motor. A relay initiates the forward drive of the variac through a reversible motor and step-down gear system. The potentiometer selects the final variac position in the range of 0–230 V. The slowly varying voltage from the variac is stepped up, rectified and is used for charging the Marx capacitors (Lali *et al* 1979). A high voltage circuit breaker driven by a motor is used to connect the power supply with the Marx. After the capacitors are charged, the motor disconnects the power supply from the Marx to prevent transients generated during Marx erection from damaging the power supply.

The Marx has a measured inductance of 6 μH while the impedance is 25 ohm when operated at 400 kV. These parameters are measured with the help of a very low inductance resistor made of copper sulphate solution and a fast current transformer (Kubota *et al* 1973 and Takagi *et al* 1979). The typical output voltage wave from the Marx is shown in figure 5.

2.2 *Coaxial water line*

The coaxial water line is the secondary energy storage which shapes and compresses the Marx output voltage pulse and hence is referred to as the pulse-forming line. While being charged by the Marx generator, it acts as a lumped capacitance, and discharges in a transmission line mode. The shape of the output pulse depends on the load which is connected across it while the duration of the pulse is decided by the length of the coaxial water line. This produces nearly an order of magnitude decrease in the pulse duration resulting in an increase in the power output. The reason for using water as a dielectric is its high dielectric constant (ϵ=80), which provides a medium capable of storing energy at a density of 160 kilo joule/meter^3. In addition, the velocity of propagation of an electromagnetic wave through water being about 9 times less than that through air, the pulse-forming line can be made quite compact (Harris & Milde 1976).

The coaxial water line used in the present device consists of an inner conductor (SS) with a diameter of 15 cm and an outer conductor (SS) with a diameter of 30 cm which corresponds to a characteristic impedance of 4·8 ohms. It can be operated upto 2 MV without electrical breakdown. The capacitance of the coaxial water line is equal to 5·5 nF, less than the Marx erected capacitance ($\approx$ 10 nF). So there will be some undesirable late time energy. The calculated rise-time of the output pulse by using this 4·8 ohm coaxial water line is 10 ns. The physical length of the line is 80 cm corresponding to nearly 50 ns output pulse duration when terminated with a matched load. Deionised water is circulated with low conductivity and the resistive discharge time for the line in the present geometry is a few microseconds, which is much greater than the time the Marx generator takes to charge the line. An external inductance of 10 μH is introduced between the Marx and the line to slow the rate of charging and hence reduces prepulse (Olson 1976). The line gets charged to peak

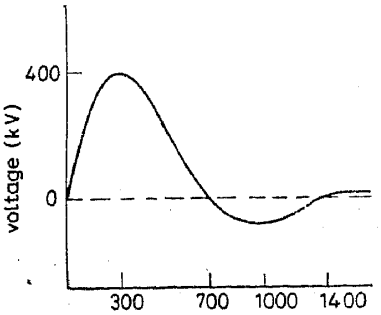

Figure 5. Marx output voltage waveform

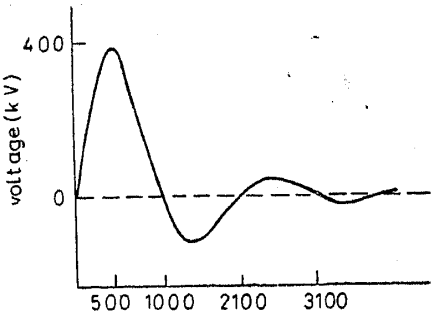

Figure 6. Water line charging voltage waveform

value in about 600 ns. The voltage pulse of the Marx which charges the water line is shown in figure 6. A thick perspex flange is used as an interface between the water line and the Marx. This flange also serves as a support for the inner conductor of the water line.

2.3 *High voltage holding switch*

The output switch connecting the coaxial water line to the load *i.e.* field emission diode is the most critical component of the REB generator. The switching of the charged pulse line into the diode requires the reliable firing of a normally insulating gap *i.e.* failure of the insulating properties of the dielectric at a predescribed location and at a predetermined time or voltage. This has been achieved by the self-breakdown of the insulating gaps.

In most beam generators, either a pressurised gas switch or a water switch is used. The breakdown strength of water depends upon duration of time in which the high voltage exceeds 63% of the breakdown strength and the area of the electrodes over which the voltage exceeds 90% of the breakdown strength. For water, E_{BD} (breakdown strength) at the positive electrode is much less than the E_{BD} at the negative electrode, a fact of considerable importance for asymmetrical configuration. According to Martin's empirical formula (Nation 1979), the breakdown strength is given by,

$$E_{(+)} = 0{\cdot}3\, T^{-1/3}\, A^{-1/10},$$

when the streamer starts from positive electrode, and

$$E_{(-)} = 0{\cdot}6\, T^{-1/3}\, A^{-1/10}$$

when the streamer starts from negative electrode, where E is in MV/cm. T, the effective time in μs is defined as the time for which the field is greater than 63% of the breakdown voltage. A is the effective area in cm^2 and is defined as the surface area on the appropriate electrode over which the field is greater than 90% of the breakdown fields.

The main disadvantage of the water switch is that the coupling capacitance between the water line and the diode increases (since capacitance is proportional to ϵ and for water ϵ=80) resulting in large prepulse amplitude.

In the present REB generator, we have tried a combination of a pressurised gas switch and a water switch, connected in series. A major advantage of using a gas switch in series with a water switch comes from its low capacitance. So the net capacitance of this combination is low, which results in decoupling of the diode from the water line during charging. This minimises the prepulse and removes a major cause of cathode emission irregularities. Also, by adjusting the pressure inside the gas switch externally, we can operate the switch at different voltages.

The gas switch is housed inside a thick perspex housing which can be pressurised upto 50 psi. The gap between electrodes is 4·5 cm. The water switch, connected in series with the gas switch, consists of brass electrodes of 30 mm diameter. The gap between the electrodes can be adjusted from 0 to 30 mm. The breakdown strength of the water switch is around 240 kV/cm. Both the switches are mounted inside a stainless steel cylinder through which deionised water is continuously circulated. The Marx output waveform when the output switch fires at the peak voltage is shown in figure 7.

2.4 *Field emission diode*

Converting the voltage pulses to electron beams requires the use of a high-voltage low-inductance field emission diode, which alone can provide the high current densities required. The diode consists of a graphite cathode and spaced from it is an anode which is either an aluminium foil or a brass grid. For a plane parallel diode consisting of a cylindrical cathode of radius R and vacuum gap d to a flat anode, the impedance is given by the Child-Langmuir relation i.e.

$$Z = 136 \frac{(d/R)^2}{\sqrt{V}},$$

where V is in MV and Z is in ohms.

The mechanism associated with electron beam generation in field emission diodes is now fairly well understood (Yonas 1974). Upon application of the electric field, microscopic projections on the cathode are heated by ohmic currents and after a few

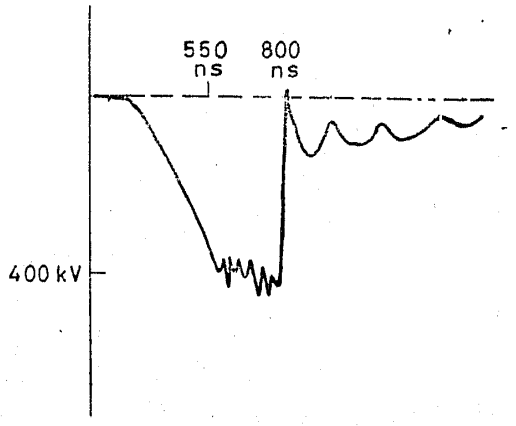

Figure 7. Marx voltage when high voltage holding switch fires.

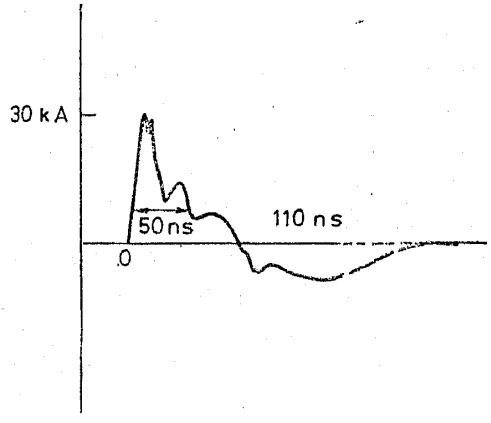

Figure 8. Field emission diode current waveform. Peak current is 30 kiloampere. Horizontal scale 100 ns per division.

nanoseconds, the projections vaporise forming a plasma sheath which emits electrons copiously. The voltage waveform applied to the diode has a very marked effect on the beam uniformity and reproducibility. A rapidly rising voltage provides whisker explosion all over the cathode surface, providing a uniform plasma. A slowly rising voltage will explode whiskers at different times in random places over the cathode surface and lead to a highly non-uniform beam. Hence fast rise-times are desirable, which in our machine are obtained by reducing the effective length of the output switch and the diode.

The aluminium foils used as anode are almost always destroyed after each shot because of the high current densities of the electron beam passing through it. This necessitated the use of a foil changer so that after each shot the foil can be replaced without opening the vacuum system. The changer consists of a modified brass flange with various gears, stretcher ring and dispenser and receiver spools fixed on it and is mounted in the anode plane of the diode. A shaft is connected to the gear system which comes out of the vacuum system through a motion feedthrough. By rotating it, we can change and stretch the foil. Foils for over 30 shots can be loaded onto the changer.

3. Diagnostic and experimental results

The most important parameter of the generator is the output current. Two self-integrated Rogowskii coils are used to monitor the diode and the net current. They are made from copper wire and mounted inside the perspex enclosures. About 60 cm length of thin wires are used to terminate the coil, and the current through these wires is measured with the help of a current transformer. These Rogowskii coils are calibrated initially by a 60 ns duration, 60 amp square pulse. It is found that their high frequency response is remarkably good while the calibrated output is 0·5 V/kA and 0·8 volt/kA respectively. One of the Rogowskii coils is mounted over the cathode to monitor the diode current while the other is placed about 5 cm away from the anode inside the drift chamber to monitor the net current.

The diode current signal obtained with a 4 cm diameter flat graphite cathode and a brass grid anode when a 200 kV pulse was applied between them is shown in figure 8 The cathode-anode spacing of 3 mm was retained. The peak current in this signal is found to be equal to 30 kiloamperes, while the duration of the pulse is 60 ns. This value of diode current agrees with the value obtained from the Child-Langmuir relation. The 10 to 90% rise-time of the pulse is equal to 10 ns and corresponds to nearly 70 nano-Henry inductance of the switch and the diode. The diode current corresponds to an electron density of 7×10^{11} cm^{-3} while the total number of particles emitted is 7×10^{14}. The background pressure in the diode as well as in the drift region was 2×10^{-4} torr and no external magnetic field was applied. The punctured aluminium foil used as anode is shown in figure 9 (plate 1).

The net current measured by the second Rogowskii coil after the anode is shown in figure 10. The value of the signal corresponds to 22 kA. It is important to note that the signal decays to zero in about 2 μs. This can be explained by the fact that due to the fast initial rise of the diode current with which large electric fields are associated (Hammer *et al* 1977), there is a breakdown of the background gas resulting in the formation of a plasma. During the fall of the diode current *i.e.* when the beam starts

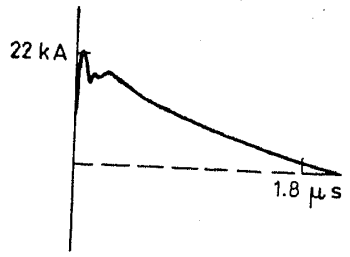

Figure 10. Net current measured by Rogowskii coil.

leaving the system, a current is induced in the plasma, flowing in the same direction as the beam and the decay of this current depends on the plasma conductivity. With the knowledge of the decay (L/R decay time$=2{\cdot}0$ μs), one can determine the plasma conductivity and hence the temperature. The plasma temperature obtained in our case is 0·6 eV. Beam propagation in the drift tube was confirmed by the damage pattern on the aluminised mylar foils kept at distances even upto 55 cm away from the anode.

We wish to thank Drs P P Rao, A M Punithavelu and P K Bhattacharjee and Mr H A Pathak for their assistance during fabrication and testing of the device. We acknowledge discussions with other members of the plasma physics group.

References

Bagratashoili V N, Knyazev I N, Kudravtsev Y A & Letokhov V S 1973 *Opt. Commun.* 9 135
Chu K R & Rostoker N 1974 *Phys. Fluids* **17** 813
Fitch R A 1971 *IEEE Trans. Nucl. Sci.* **NS-18** 190
Grabill S E & Uglum J R 1970 *J. Appl. Phys.* **41** 236
Hammer D A, Robson A E, Gerber K A & Selhian J D 1977 *Phys. Lett.* **A60** 31
Harris N W & Milde H 1976 *IEEE Trans. Nucl. Sci.* **NS-23** 1470
Kobota Y, Kawasaki S, Miyahara A & Saad H M M 1973 Nagoya University Tech. Report
Lali K S, Pujara H D & Saxena Y C 1979 Physical Research Laboratory, Technical Note No. TN-79-03
Molvig K & Rostoker N P 1977 *Phys. Fluids* **20** 494
Nation J A 1970 *Appl. Phys. Lett.* **21** 491
Nation J A 1979 Cornell University Report No LPS-263
Olson N T 1976 Unpublished report
Oswald R B Jr, Eisen R A & Conrad E E 1966 *IEEE Trans. Nucl. Sci.* **NS-13** 229
Prestwich K R 1971 *IEEE Trans. Nucl. Sci.* **NS-18** 493
Sandel F L 1973 Cornell University Report No. LPS-131
Takagi K, Kabota Y & Miyahara A 1979 *Jpn. J. Appl. Phys.* **18** 1135
Yonas G 1974 *Nucl. Fusion* **14** 731

Plate 1

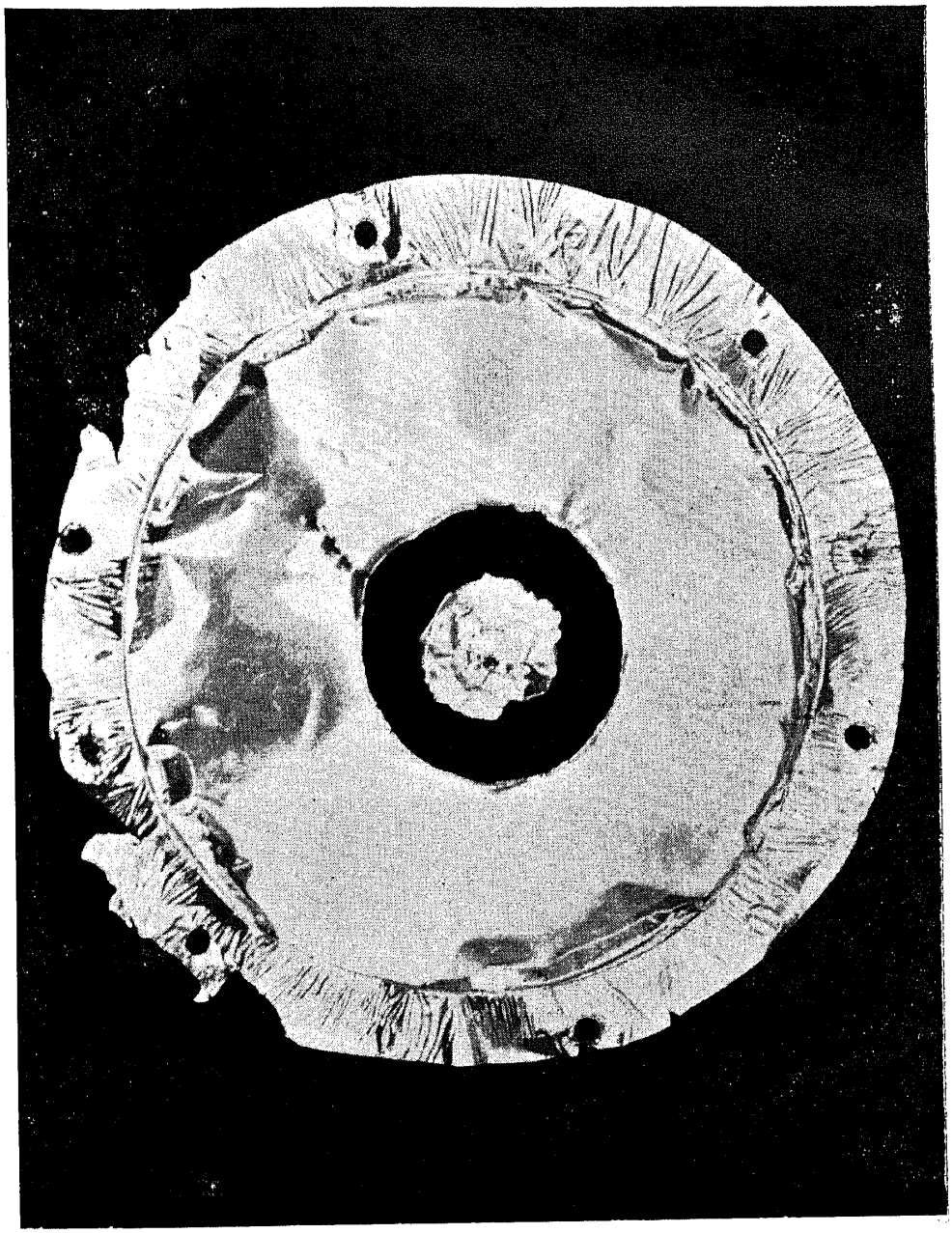

Figure 9. Punctured 17 μm thick aluminium foil used as anode.